# EXPERIMENT OF CUSPTRON MICROWAVE TUBE

J. Y. Choe, K. Boulais, H. S. Uhm
*Naval Surface Warfare Center*
*White Oak, Silver Spring, Maryland 20903–5000*

W. Namkung
*Pohang Institute of Science and Technology*
*Pohang, Korea*

## Abstract

The cusptron microwave tube is a compact high power device using the harmonic frequency generating scheme via the negative mass instability with an axis–rotating electron beam. Both the high and low harmonic modes of operation in the oscillator configuration have been successfully demonstrated and the beam dynamics have been studied to improve beam quality. The program is now in preparation for conversion of the cusptron into an amplifier configuration.

## Introduction

The object of the cusptron program at the Naval Surface Warfare Center (NSWC) is to develop a compact and high power microwave amplifier based on the cusptron concept[1-3]. High power microwave and millimeter–wave sources are in great demand for practical applications in particle accelerators, communications, radars, plasma heating, and many other systems.

The cusptron microwave tube is a compact high power device utilizing harmonic frequencies by the negative mass instability of an axis–rotating beam, created by injection through a magnetic cusp. The electron beam, during its cyclotron motion, becomes azimuthally bunched by the instability and interacts with the RF modes to produce harmonics of the cyclotron frequency. Different RF circuits are utilized depending on the harmonic number desired. Thus, two mode of operations are possible for the cusptron: (1) the high harmonic mode with a multi–vaned circuit to encourage high azimuthal mode numbers, and (2) the low harmonic mode of operation with the usual smooth cylindrical wall. In addition to this difference in the RF circuits, the optimum beam parameters are also different, and careful beam shaping with the magnetic field is necessary.

## High Harmonic Mode Oscillator

The experimental setup of the cusptron oscillator configuration is schematically shown in Fig. 1. The magnetic cusp is produced by opposing magnetic fields on either side of highly permeable soft iron pole plate. A hollow electron beam is produced from an annular thermionic cathode, and in passing through the narrow field reversal region, the azimuthal impact of $v_z \times B_r$ forces the electrons to rotate about the axis in the downstream

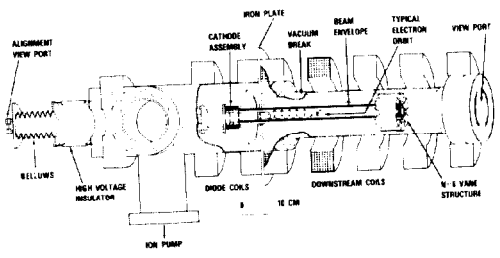


*Fig. 1. Schematic of the experiment for high harmonic mode operation.*

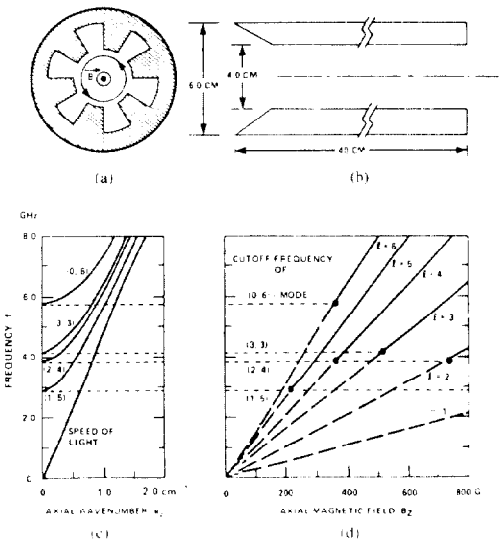


*Fig. 2. Characteristics of multivane circuit. (a) Cross section and (b) dimensions of the six–vane circuit, (c) dispersion curves and (d) beam–wave interaction region in magnetic fields.*

region. The electron energy is provided by a high voltage modulator of up to 30 kV, 5 A, 1 kHz PRF, 10 $\mu$s PW.

For the high harmonic mode of operation, a six–vane structure was used in the interaction region, as shown in Fig. 1. The vane structure is employed to encourage a particular RF mode[4], for example, the (0,6)–mode to couple with six beam bunches. The periodic interruption on the wall groups the azimuthal mode number in a distinctive way, so that a particular azimuthal mode number can be selected[4]. The cross section and dimensions of the six–vane circuit are shown in Fig. 2 along with vacuum dispersion relations and the magnetic fields needed for beam–wave interaction. In order to be synchronous, the magnetic field strength [Fig. 2(d)] has to be such that its beam mode, $\ell\omega_c$, is equal to or greater than the corresponding RF cutoff frequency [Fig. 2(c)]. This is shown by the solid lines in Fig. 2(d).

The experiment was operated at 25–30 kV, 4 $\mu$s PW, 60 Hz PRF, and 0.1–1.0 $\mu$perv. The applied magnetic field was 180–270 G in the diode region and 340–490 G in the interaction region. Radiation was detected by a C–horn antenna, and the RF diagnostic system included a spectrum analyzer to accurately monitor its frequency and mode purity. By adjusting the magnetic field, two nearby operating regimes were found. One produced 10.0 kW of power at 6.0 GHz, and the other yielded 4.0 kW at 3.9 GHz corresponding to the sixth and fourth harmonics of cyclotron frequency, respectively. The electronic efficiencies were approximately 10% for both. The mode purity for the two outputs is clearly demonstrated from the spectrum analyzer traces in Fig. (3) and (4) for the sixth and fourth harmonics, respectively. The center frequency is 6.0 GHz with 0.5 GHz/div and 10 dB/div in both traces showing no mode competition within the 60 dB dynamic range.

CH2669-0/89/0000-0091$01.00©1989 IEEE

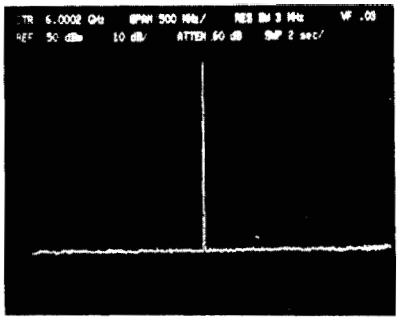

*Fig. 3. Spectrum Analyzer trace for sixth harmonic frequency generation.*

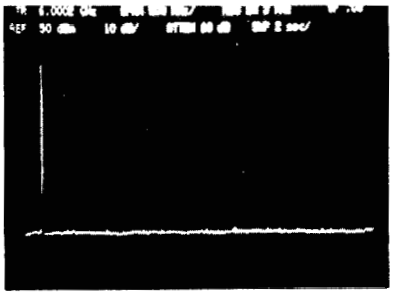

*Fig. 4. Spectrum Analyzer trace for fourth harmonic frequency generation.*

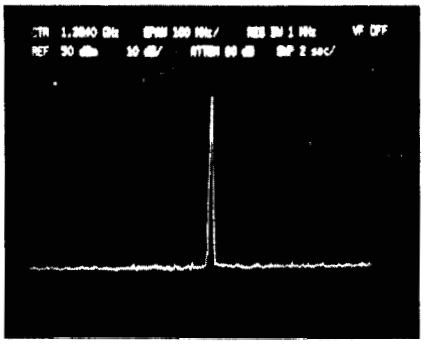

*Fig. 5. Spectrum Analyzer trace for fundamental frequency generation.*

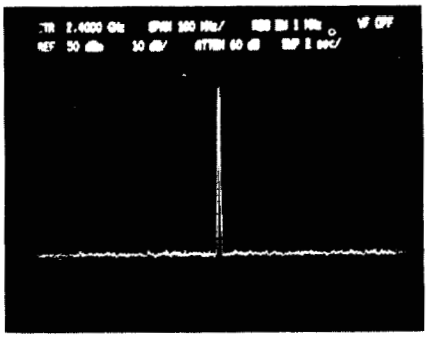

*Fig. 6. Spectrum Analyzer trace for second harmonic frequency generation.*

### Low Harmonic Mode Oscillator

For the low harmonic mode of operation, the six–vane circuit has been removed and a smooth cylindrical tubing of 7.41 cm radius served as the cavity. The Rf modes interacting with the beam were $TE_{11}$ and $TE_{21}$ producing the fundamental and second harmonics of the cyclotron frequency. As in the case of the high harmonic operation, these two modes are separated by different magnetic field strength. Further examination of the magnetic field revealed that beam compression was necessary to locate the beam at the optimum field strength. This was in contrast to the high harmonic case, where the beam should be located close to the wall.

In the fundamental cyclotron frequency generation, the $TE_{111}$ and $TE_{112}$ modes were separately excited by adjusting the magnetic field. The observed frequencies were 1.266 GHz and 1.384 GHz at 1.8 kW output. Again, as Fig. 5 indicates, the mode purity was found to be excellent. In the second harmonic generation case, the $TE_{211}$ and $TE_{212}$ modes are separately excited at 2.24 and 2.40 GHz, respectively, at 1.8 kW output. The mode purity is again evident from Fig. 6 where the spectrum analyzer trace for the second harmonic is shown.

### Beam Dynamics Study

Although production of an axis–rotating electron beam (e–layer) by magnetic cusp injection is superior in simplicity and beam quality, an ideal beam can only be realized by utilizing an ideal cusped field. An ideal e–layer has no variations in beam guiding radius along the axis of propagation (orbit off–centering) and no spread in axial velocity ($\Delta v_z$). A realistic beam invariably has these undesirable effects, and thus, we have studied the beam dynamics both theoretically and experimentally.

The major sources of orbit off–centering of the electron beam in the cusptron include: (1) a finite cusp transition region (finite span), (2) an unbalanced magnetic field reversal, and (3) a finite Larmor radius before the beam enters the cusp (upstream region). Theory has shown[5] that an unbalanced cusp will dominate the orbit off–centering and the other two effects are only significant for the balanced cusp. The originating source of $\Delta v_z$ is from the finite radial thickness of the cathode but the spread can increase from the off–centering sources.

In the experiment, as shown in Fig. 7, a phosphor screen was used to measure beam radius and rotational velocity (relative to axial velocity) as a function of axial distance, $z$. The velocity ratio, $\alpha$, was measured by using a stainless steel strip placed 0.5 cm in front of the phosphor. The strip imposed a shadow on the phosphor at an azimuthal location proportional to the pitch angle of the electron beam. The beam parameters were measured for several different field configurations.

The unbalanced field shown in Fig. 8(a) is similar to the configurations used for the high and low harmonic microwave production. This type of field was used because the upper limit of our high voltage modulator imposed a limit on the electron accelerating voltage. Since the downstream field is fixed by microwave frequency, a larger upstream field needed for a balanced cusp would prevent electron penetration into the downstream region.

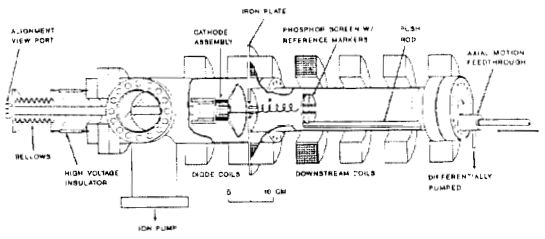


*Fig. 7. Schematic of experimental setup for the beam dynamics study.*

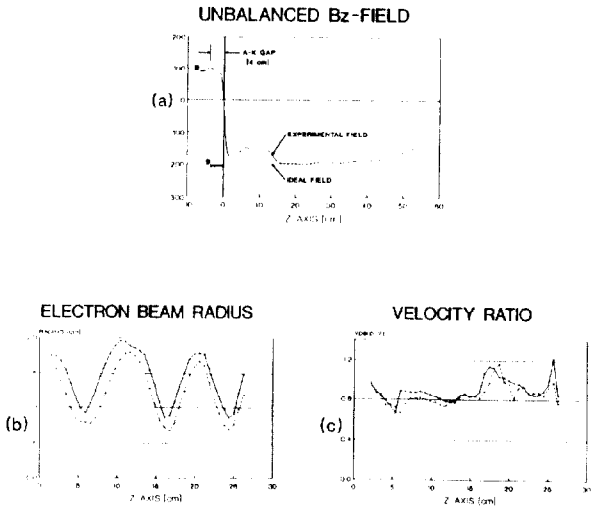


*Fig. 8. Unbalanced cusp field experiment. (a)The axial magnetic field profile, (b) electron beam envelope, and (c) the velocity ratio $\alpha$ are shown.*

However, the large amount of orbit off–centering in such a configuration is evident from the oscillations shown in the beam envelope of Fig. 8(b). In Fig. 8(c), one notes the large variations in $\alpha$ as the beam propagates along the axis.

By inserting an adiabatic compression stage between the cusp and the downstream region [Fig. 9(a)], several advantages become apparent. First, a low electron accelerating voltage can be realized since the overall field magnitude on either side of the cusp is reduced. Second, a balanced cusp can be utilized deleting the major source of orbit off–centering. Third, the finite transition source of off–centering is reduced since the electrons will penetrate the cusp with a higher axial velocity[6]. Finally, any other source of off–centering will be reduced in proportion to the reduction of beam radius. Such a reduction in off–centering can be seen in the radial data of Fig. 9(b). Even though the upstream and downstream field magnitude is the same as for the unbalanced configuration, the beam off–centering and spread in axial velocity [Fig. 9(c)] has been reduced by a factor of two.

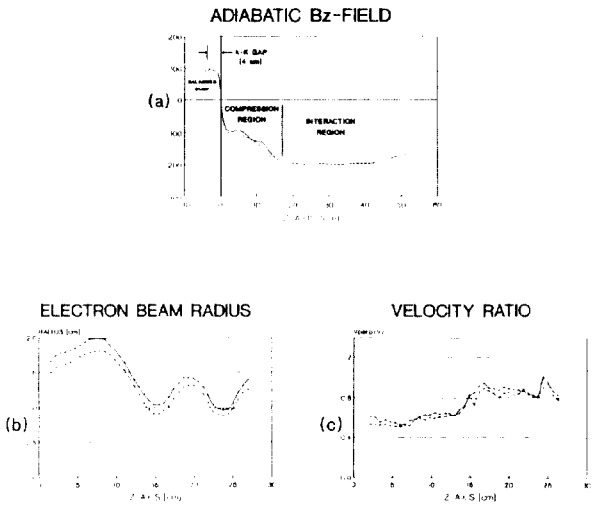


*Fig. 9. Adiabatically compressed balanced field experiment. (a)The axial magnetic field profile, (b) electron beam envelope, and (c) the velocity ratio $\alpha$ are shown.*

## Cusptron Amplifier Configuration

The NSWC cusptron oscillator is now undergoing conversion to an amplifier. The proposed amplifier configuration is depicted in Fig. 10. The input signal to the cusptron comes from a 1 kW TWT with a frequency range of 4–8 GHz. The TWT is pulsed in synchronism with the high voltage cathode pulse through a sync pulse generator of variable PRF and variable PW. The high voltage modulator will be operated up to 50 kV. The output of the cusptron amplifier will be connected to a group of diagnostic including a spectrum analyzer to accurately monitor the frequency and its stability, a power meter to measure relative gain and absolute power, and phase detectors to measure phase stability of the output relative to the input.

The input and output couplers in the cusptron are small, single–turn loop antennas. The output couplers are connected from the end plate, and the input wave is carried to its coupler via rigid coaxial cable through the vacuum. In order to help identify the modes of the produced microwaves, several output couplers are provided at different azimuthal locations.

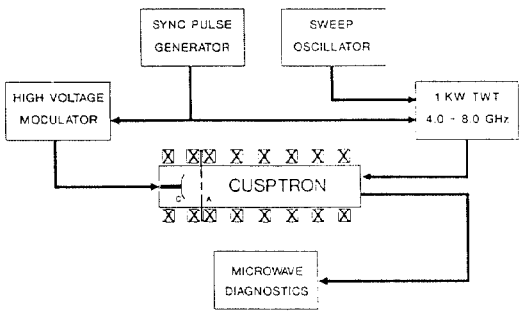


*Fig. 10. Block diagram of cusptron amplifier system setup.*

## Conclusion

We have reported the successful results of the cusptron oscillator and emphasized its superior quality in the mode purity and the frequency stability. Then we discussed our plan to convert it to an amplifier configuration, and in the preparation process we have investigated the beam dynamics. We have concluded that the off–centering due to the unbalanced cusp is very harmful and the staged field profile featuring a balanced cusp and an adiabatic compression phase is desirable.

## Acknowledgement

This work is supported by the Independent Research Fund at the Naval Surface Warfare Center.

## References

1. W. Namkung, Phys. Fluids 27, 329 (1984).
2. H. S. Uhm, C. M. Kim, and W. Namkung, Phys. Fluids 27, 488 (1984).
3. W. Namkung and J. Y. Choe, IEEE Trans. Nucl. Sci. NS–32, 2885 (1985).
4. J. Y. Choe, V. Ayres, W. Namkung, and H. Uhm, Int. J. Electronics, 6, 389 (1988).
5. J. Y. Choe, K. Boulais, E. H. Choi, W. Namkung, V. Ayres, and H. Uhm, "Beam Dynamics of Cusp Produced Axis–Encircling Beam," manuscript in preparation (1989).
6. K. Boulais, J. Y. Choe, E. H. Choi, W. Namkung, V. Ayres, and H. Uhm, "Experimental Study of Axis–Encircling Beam by Cusp Injection," manuscript in preparation (1989).